Organic & Biomolecular Chemistry

Accepted Manuscript

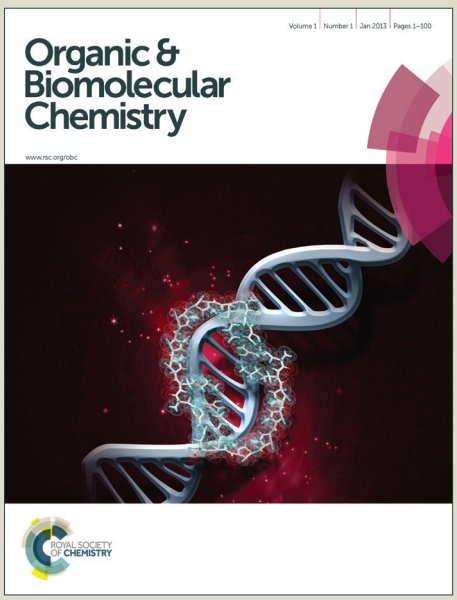

ROYAL SOCIETY OF CHEMISTRY

www.rsc.org/obc

The Role of Ammonia Oxide in the Reaction of Hydroxylamine with Carboxylic Esters

Carlos M. Silva, Isabela C. Dias and Josefredo R. Pliego Jr.*

Departamento de Ciências Naturais, Universidade Federal de São João del-Rei
36301-160, São João del-Rei, MG, Brazil.

* pliego@ufsj.edu.br

Abstract

Theoretical calculations indicates that hydroxylamine can exist in the both neutral and zwitterionic (ammonia oxide) forms in aqueous solution, the former being 3.5 kcal mol^{-1} more stable. In this report, we have studied the reaction mechanism of hydroxylamine with phenyl acetate and analyzed the role of zwitterionic isomer. We have observed that the main reaction pathway takes place through the zwitterionic form with a concerted mechanism, not involving the classical tetrahedral intermediate. Attack by the nitrogen atom (via neutral isomer) has a minor contribution and it is also a concerted process. The activation free energy barriers in aqueous solution were calculated at MP4/TZVPP+diff level for gas phase energies, CPCM for optimization and frequencies, and through single point calculation of the solvation free energy using the SM8 method. Our theoretical predicted barriers are 20.8 and 23.8 kcal mol^{-1} for O and N attack, respectively, in very good agreement with the experimental values of 20.4 and 22.3 kcal mol^{-1}, respectively. Our results support the view that hydroxylamine is a very special nucleophile and the reactivity of this functional group should be further investigated.

Keywords: ab initio, α-nucleophile, organocatalysis, nucleophilic catalysis, bifunctional catalysis, ester cleavage, solvent effect.

Introduction

In a set of two papers published in 1958, Jencks reported that hydroxylamine reacts with *p*-nitrophenyl acetate to form *O*-acylhydroxylamine as the main product and a low proportion of hydroxamic acid.[1, 2] This observation was intriguing because it is known that nitrogen nucleophiles are more reactive than oxygen nucleophiles. Jencks suggested three mechanisms involving formation of the tetrahedral intermediate, shown in Scheme 1. The first possibility would be the involvement of the zwitterionic form of hydroxylamine, with nucleophilic attack of the oxygen atom and stabilization of the developing charge on the carbonyl oxygen through hydrogen bond (I). The second possibility would be nucleophilic attack of the oxygen atom with hydroxylamine in the neutral form (II). The third pathway is similar to (II), but it involves the simultaneous proton migration from oxygen to nitrogen of hydroxylamine (III).

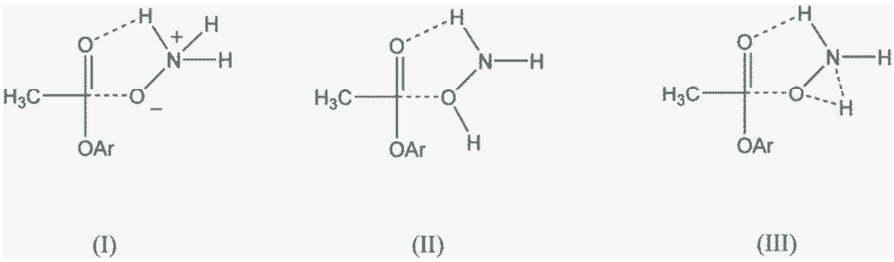

Scheme 1: Possible mechanisms proposed by Jencks**.**

Hess, Hengge and Cleland have used isotopic effect to reinvestigate the reaction of hydroxylamine with *p*-nitrophenylacetate[3]. Their analysis suggests the mechanism is compatible with the formation of the tetrahedral intermediate and its breakdown is the rate determining step. In addition, those authors have proposed that the first step is the mechanism (III) in Scheme 1. More recently, Mazera et al have reported kinetic studies on the reaction of hydroxylamine with five different derivatives of phenylacetate.[4] For phenylacetate, p-chlorophenylacetate and p-nitrophenylacetate, first and second order kinetics in hydroxylamine (second and third

order global, respectively) were observed. These results point out that both bimolecular (one hydroxylamine) and termolecular (two hydroxylamines) mechanisms play a role in this reaction. Posterior theoretical studies at B3LYP/6-311+G(2df,2p)//HF/6-31G(d) level of theory and including solvent effect at PCM/HF/6-31G(d) level was used to explore different reaction mechanisms involving the tetrahedral intermediate formation.[5] The investigated bimolecular mechanisms have considered direct attack of the hydroxylamine nitrogen or oxygen atoms with simultaneous proton transfer to the carbonyl (Scheme 2). The calculated free energy barriers were very high, around 50 kcal mol^{-1}. Bifunctional catalysis by a water molecule was also considered and although the barriers have decreased to 30 kcal mol^{-1}, this mechanism does not explain the experimental kinetics with free energy barriers of 20 kcal mol^{-1}. Therefore, previous theoretical studies have not found a reaction pathway able to explain the bimolecular mechanism.

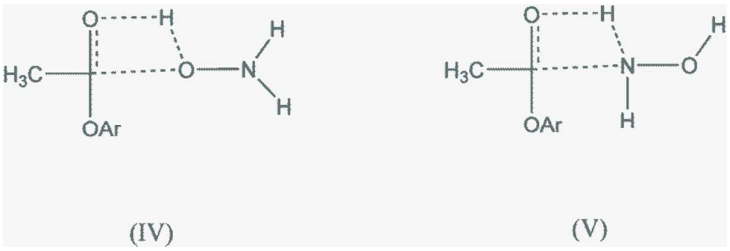

Scheme 2: Bimolecular reaction mechanisms investigated by Mazera et al[5].

Unexpected results from previous investigations were the discovered of the catalyzed mechanisms. Mazera et al[4, 5] have found that hydroxylamine can acts as a bifunctional catalysts involving the oxygen and nitrogen atoms simultaneously. The nitrogen atom acts as a base, receiving a proton of the attacking nucleophilic atom whereas the oxygen atom acts as an acid, making hydrogen bond with the carbonyl oxygen and transferring the proton. Thus, there is formation of a complex involving the tetrahedral intermediate and hydroxylamine in the zwitterionic form. In the next step, the $-NH_3^+$ group moves to the phenoxide oxygen and induces the breakdown of the tetrahedral intermediate. The mechanism is presented in Scheme 3 and it was found it

has low free energy barrier, around of 20 kcal mol^{-1}, explaining the experimental findings.

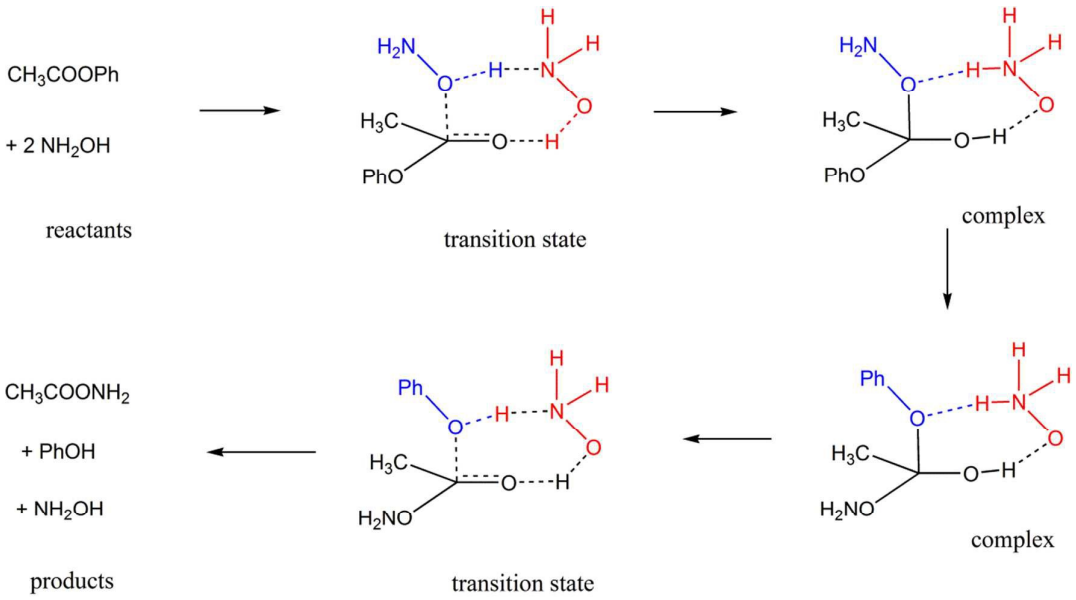

Scheme 3: Dual Bifunctional Catalysis mechanisms investigated by Mazera et al[5].

The role of the zwitterionic form of hydroxylamine, which should be more reactive than the neutral form, depends on its stability. If the reaction leading to the zwitterionic form has high free energy, this species should not be kinetically relevant. This problem has been addressed by Kirby et al[6] through *ab initio* methods coupled with continuum, discrete-continuum and free energy perturbation with classical force-field. The uncertain in the stability of the zwitterionic form was as large as 15 kcal mol^{-1}, with the zwitterionic form being more or less stable than the neutral form depending on the solvation model. In a later report, Kirby et al[7] have used empirical relations to propose that the neutral isomer is only 0.9 kcal mol^{-1} more stable than the zwitterionic form. A theoretical analysis by Fernandez et al has found the neutral form is 2.2 kcal mol^{-1} more stable than the zwitterionic isomer.[8] The most recent study by Lima et al[9] using Shells Theory of Solvation (STS)[10, 11] has predicted the neutral form is 3.5 kcal

mol^{-1} more stable. In that study, several continuum solvation models and parametrizations were tested and it was found the SM8 and SM8AD methods are able to reproduce the most sophisticated STS method.

Some recent papers have emphasized the role of the zwitterionic form of hydroxylamine in the reactions with phosphate esters[12] and sulfonamides[13]. The previous studies by Mazera et al[4, 5] related to reactions with carboxylic esters have not included a bimolecular mechanism involving the zwitterionic form of hydroxylamine. In fact, any reliable theoretical study should make use of a solvation model able to predict correctly the stability of the zwitterionic form. Otherwise, the free energy barrier could not be sound. The aim of this paper is to elucidate the role of zwitterionic form of hydroxylamine in the reaction with phenyl acetate in aqueous solution and finding the mechanism able to explain the bimolecular process.

Computational Methods

The search for minima and transition states has been done using density functional theory with the X3LYP functional[14, 15] and the 6-31(+)G(d) basis set, which corresponds to 6-31G(d) basis set for carbon and hydrogen and 6-31+G(d) basis set for oxygen and nitrogen. In order to refine the geometries, we have done more optimizations including the solvent effect (water) through the CPCM method.[16] Following these optimizations, we have done harmonic frequency calculations to compute the vibrational, rotational and translational contributions to the free energy in both gas phase and solution phase. These calculations in liquid phase were done using the CPCM/X3LYP/6-31(+)G(d) method and tesserae numbers of 60 and 240. Analysis of our results have indicated a sensible value of free energy obtained in the frequency calculations, suggesting that 60 and even 240 tesserae does not produce accurate frequencies due to numerical error. Therefore, we have done more refined CPCM frequency calculations with 960 tesserae for reactants, TS1 and TS3 structures, while using liquid phase geometries and gas phase frequencies for determining all the free energy profile.

Connection between minima and transition states was confirmed through Intrinsic Reaction Coordinate (IRC) calculations in gas phase. Higher level electronic energies were obtained at single point calculations using MP2/6-31(+)G(d), MP4/6-31(+)G(d) and MP2/TZVPP+diff electronic structure methods. The TZVPP+diff basis set corresponds to the def2-TZVPP basis set of Ahlrichs and co-workers supplemented by diffuse sp functions on oxygen and nitrogen atoms[17]. The additivity approximation was used to obtain effective MP4/TZVPP+diff energies. The solvent contribution to the free energy was computed using the SM8/B3LYP/6-31G(d) method[18]. Thus, the final free energy for each species X in solution was calculated through:

$$G^*_{sol}(X) = G_{el}(X) + G_{vrt}(X) + \Delta G_{solv}(X) + 1.89 \text{ kcal/mol}$$

where $G_{el}(X)$ is the electronic energy calculated at MP4/TZVPP+diff level, the $G_{vrt}(X)$ is the vibrational, rotational and translational contributions to the free energy obtained from the gas or solution phase frequency and $\Delta G_{solv}(X)$ is the solvation free energy obtained from the single point SM8 calculations. The 1.89 kcal/mol term is the correction from 1 atm to 1 mol/L standard state.[19]

In order to analyze the gas phase and solvation contribution, we have also defined the gas phase free energy as:

$$G^*_{g}(X) = G_{el}(X) + G_{vrt}(X) + 1.89 \text{ kcal/mol}$$

Thus, we have the relation:

$$G^*_{sol}(X) = G^*_{g}(X) + \Delta G_{solv}(X)$$

This is essentially the equilibrium solvation path (ESP) theory of reactions in a liquid for the case of using CPCM frequencies.[20, 21] All the calculations were done using the Firefly,[22] Gamess[23] and Gamessplus[24] programs.

Results and Discussion

The high stability of the zwitterionic form of hydroxylamine is a very interesting property of this molecule. We could wonder if similar species like hydrazine and

hydrogen peroxide could also present this property. Thus, we have used the same level of theory to study the zwitterionic form of hydroxylamine, hydrazine and hydrogen peroxide. The results are presented in Scheme 4. As we can notice, both the zwitterionic forms of hydrazine and hydrogen peroxide are much less stable than the neutral form, with liquid phase isomerization free energy higher than 25 kcal mol^{-1}. On the other hand, hydroxylamine is a very special molecule, because its zwitterionic form is predicted to be only 3.0 kcal mol^{-1} less stable than the neutral form, a value in very good agreement with previous report of 3.5 kcal mol^{-1}.[9] Therefore, there is not double that the zwitterionic form should play an important role in reactions of hydroxylamine.[25, 26] On the other hand, this unfavorable isomerization of hydrazine and hydrogen peroxide should result in less reactivity.[27]

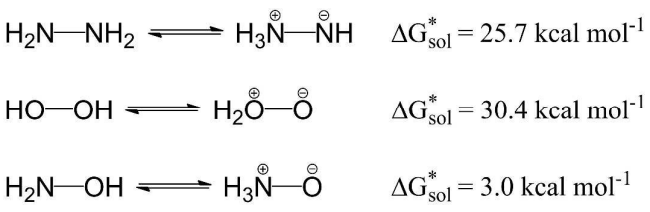

Scheme 4: Relative stability of neutral and zwitterionic forms in aqueous solution obtained at MP4/TZVPP+diff//CPCM/X3LYP/6-31(+)G(d) level and single point solvation free energy calculation at SM8 level.

In the investigation of the reaction mechanisms, we have considered the possibility of the formation of the tetrahedral intermediates as well as the direct single step mechanisms (Scheme 5). The first reaction pathway we have analyzed is the direct attack of the neutral form of hydroxylamine to the carbonyl carbon, leading to the formation of the N–C bond (hydroxamic acid + phenol). Figure 1a presents the IRC calculation and Figure 2 shows the geometrical details of the transition state TS1. As it can be noticed, we have found a reaction pathway for the direct nucleophilic attack of the hydroxylamine's nitrogen with simultaneous proton transfer from hydroxylamine's oxygen to the leaving phenoxide ion. Based on Table 1, high level of theory predicts

the gas phase free energy barrier is high, 31.6 kcal mol^{-1}. Nevertheless, the solvent effect is very important, decreasing the barrier to 23.2 kcal mol^{-1}.

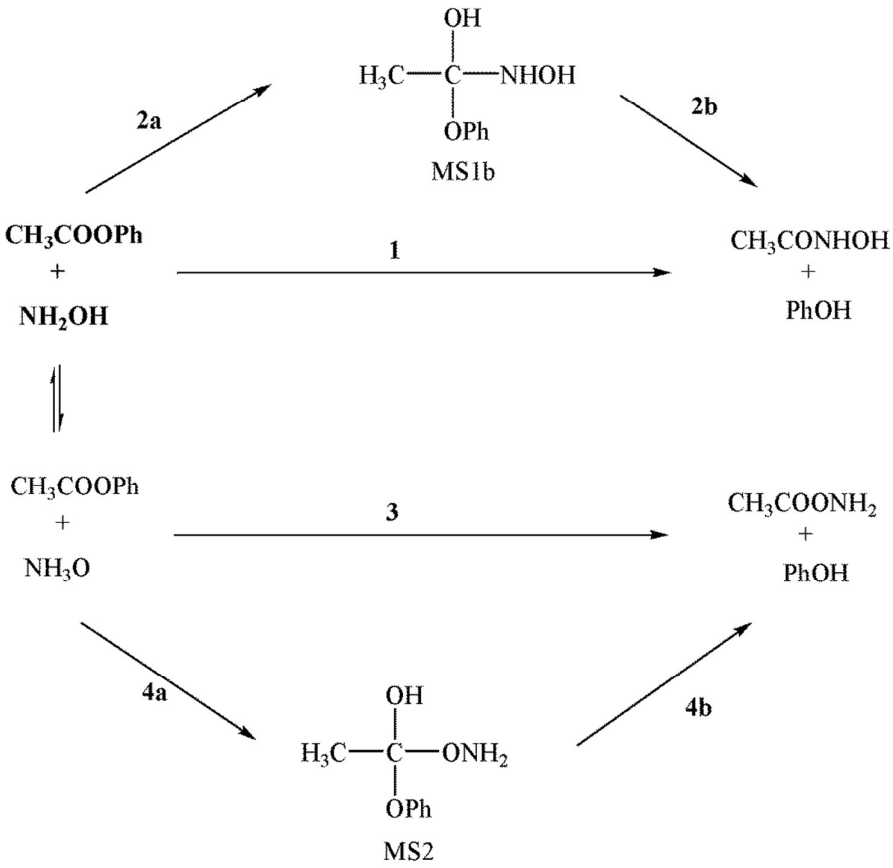

Scheme 5: Investigated reaction pathways.

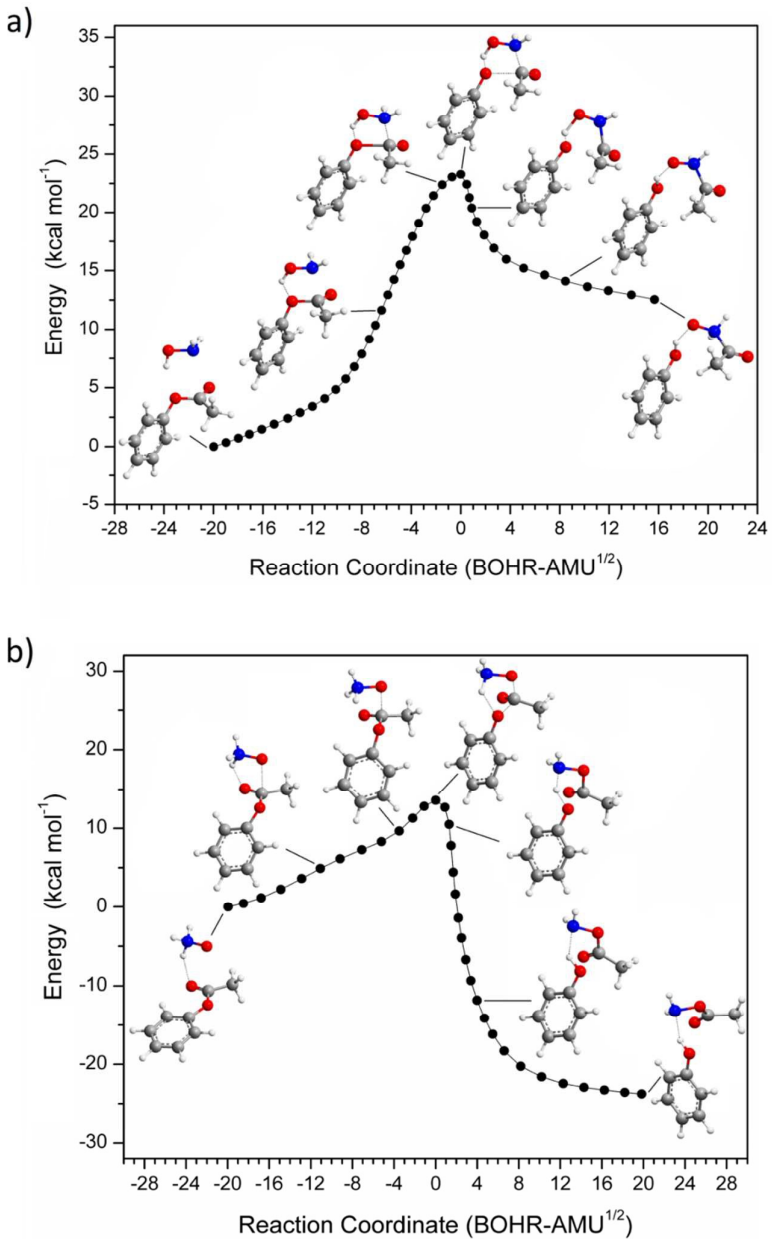

Figure 1: IRC calculations at X3LYP/6-31(+)G(d) level for the two main reaction pathways involving TS1 (a) and TS3 (b).

TABLE 1. Thermodynamics data for the hydroxylamine reaction with phenyl acetate in aqueous solution.[a]

	MS1a	MS1b	MS2	TS1	TS2a	TS2b	TS3	TS4a	TS4b
CPCM/X3LYP/6-31(+)G(d)	14.46	8.88	5.74	23.16	17.03	27.17	21.04	16.43	38.31
MP2/6-31(+)G(d)	12.38	-1.19	-4.39	22.23	13.11	30.18	24.11	14.83	47.76
MP2/TZVPP + diff	12.42	-3.70	-4.72	20.75	10.71	24.54	25.29	13.48	41.09
MP4/6-31(+)G(d)	13.26	-0.21	-3.86	22.30	14.93	29.96	23.98	16.38	46.82
MP4/TZVPP + diff[b]	13.29	-2.72	-4.19	20.81	12.54	24.32	25.16	15.04	40.15
ΔG_g^{*}[c]	26.63	10.85	9.61	31.61	23.63	33.85	37.35	26.60	47.86
$\Delta\Delta G_{solv}^{*}$[d]	-7.44	1.33	2.36	-8.42	-5.21	-7.23	-15.61	-8.53	-5.51
ΔG_{sol}^{*}[e]	19.19	12.18	11.97	23.20	18.42	26.63	21.74	18.07	42.36

[a]All energy and free energy values (CPCM, MP2 and MP4) in relation to reactants hydroxylamine (neutral isomer) and phenyl acetate. Energies in kcal mol^{-1}, [b]Energies obtained by the additivity approximation; [c]Gas-phase free energies at T=298.15 and 1 mol L^{-1} standard state; [d]Solvation free energy contribution obtained at the SM8/B3LYP3/6-31G(d) level; [e]Solution phase (water) free energies at 1 mol L^{-1} standard state.

The other reaction pathway is the O-attack involving the zwitterionic form of hydroxylamine. Figure 1b shows the IRC calculations. The zwitterionic hydroxylamine approaches the phenyl acetate through interaction of the carbonyl carbon with the hydroxylamine oxygen, while a strong hydrogen bond takes place between the hydrogen of the $-NH_3^+$ group with the carbonyl oxygen. Somewhat surprising, along the reaction pathway the $-NH_3^+$ group rotates and forms a hydrogen bond with the oxygen of the phenoxide group, facilitating the elimination of phenol via proton transfer. This transition state (TS3 in Figure 2) has a gas phase free energy barrier of 37.4 kcal mol^{-1}. The solvent effect on this highly polar transition state is very high, decreasing the barrier by 15.6 kcal mol^{-1} and leading to the final free energy barrier of only 21.7 kcal mol^{-1}.

Usual mechanisms for reactions involving the carbonyl group take place through nucleophilic attack to the carbonyl group with formation of tetrahedral intermediate. Thus, it is a surprise that the hydroxylamine presents a low barrier for a mechanism without tetrahedral intermediate formation. Nevertheless, we have also explored mechanisms involving the formation of these classical intermediates. The first possibility is the attack of the nitrogen atom of hydroxylamine to the carbonyl group with simultaneous proton transfer to the carbonyl oxygen (TS2a in Figure 2), leading to

formation of MS1a. The corresponding free energy barrier is 18.4 kcal mol^{-1}. The MS1a species is a zwitterion and its free energy is slightly above of the TS2a, 19.2 kcal mol^{-1}. This effect is due the low stability of this species (shallow minimum) and the proton vibration contribution present in MS1a and absent in TS2a. Considering the possibility of fast proton transfer from nitrogen to the medium, following back to the oxygen, the process leads to formation of MS1b, with a free energy of 12.2 kcal mol^{-1}. The following step is TS2b, resulting in elimination of phenol and formation of hydroxamic acid. The predicted free energy barrier is 26.6 kcal mol^{-1}, around 3.4 kcal mol^{-1} higher than TS1. Therefore, this pathway should not be important in the reaction. An overall view of the possible mechanisms and the corresponding free energies are shown in Figure 3. We can observe that the step for hydroxylamine isomerization to zwitterionic form is included, leading to the pathways through TS3 and TS4a.

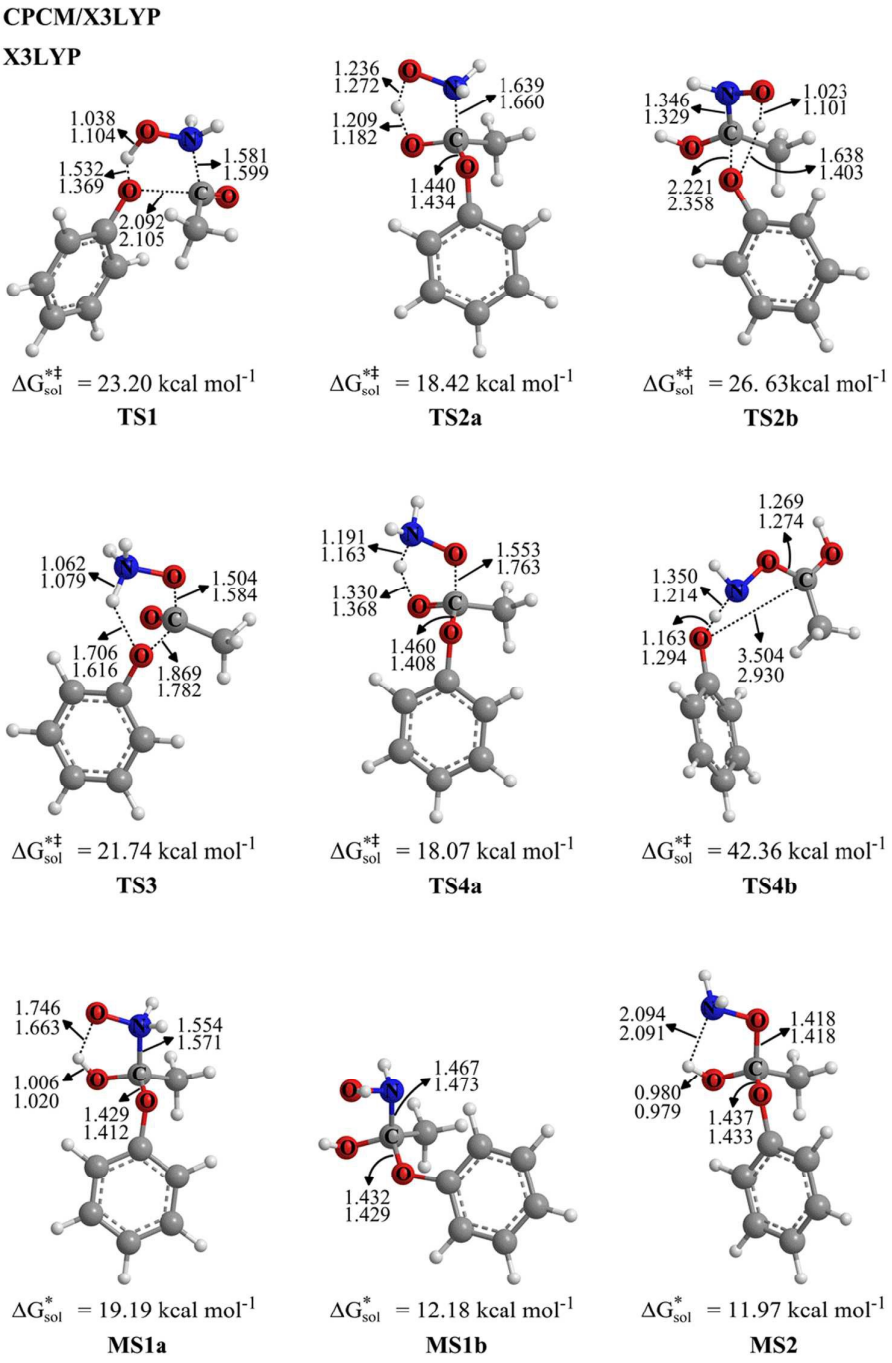

Figure 2: Minimum and transition states structures. Solution phase free energy values in relation to ester plus hydroxylamine (neutral isomer).

Other possibility involving the tetrahedral intermediate formation is the attack of the zwitterionic form of hydroxylamine, via TS4a, and formation of MS2. In the

process, there is proton transfer and the resulting MS2 is not a zwitterion. The activation free energy barrier is also low, only 18.1 kcal mol^{-1}, and the MS2 tetrahedral intermediate is 12.0 kcal mol^{-1} above of the reactants. The last step is TS4b, which corresponds to phenol elimination, with overall free energy barrier of 42.4 kcal mol^{-1}, a very high value. This difference in relation to TS2b can be attributed to less acidity of the $-NH_2$ group in relation to $-OH$ group. Consequently, this very high barrier makes this reaction pathway unviable.

A point we should comment is the possibility of water molecules to act as a catalyst to decompose the tetrahedral intermediate. Our previous report has indicated that explicit water molecules can facilitate the hydroxylamine attack to the carboxylic ester.[5] However, the barrier is very high and not competitive. Furthermore, the special structure of the tetrahedral intermediates like MS1b and MS2 suggests –OH and $–NH_2$ groups can act more efficiently than explicit water, because no entropic cost will be involved.[28]

Based on our results, the reaction of hydroxylamine with phenyl acetate takes place thought two pathways: TS1 and TS3. Both the mechanisms are single step, without tetrahedral intermediate formation. The former corresponds to N-attack and the later corresponds to O-attack. The free energy barriers are 23.2 and 21.7 kcal mol^{-1}, respectively, indicating that O-attack is the major pathway. These theoretical barriers are in very good agreement with the experimental values of 22.3 and 20.4 kcal mol^{-1}, respectively.[4] We can notice the overall kinetic barriers (theoretical and experimental) differ by only 1.3 kcal mol^{-1}, while the relative barriers are 1.5 kcal mol^{-1} (theoretical) and 1.9 kcal mol^{-1} (experimental). Therefore, the present theoretical study presents a very reliable picture of this reaction system.

A point that deserves comment is the experimental study of Hess et al[3] on the kinetic isotope effect in the reaction of hydroxylamine with *p*-nitrophenyl acetate. The neutral solvent deuterion kinetic isotope effect reported was 1.4, indicating the role of the break of hydrogen bond in the transition state. In the same way, the phenoxide's oxygen isotope effect was high, suggesting the break of oxygen-carbon bond and

release of the phenyl group in the rate determining step. The transition state TS3 is compatible with both of these effects.

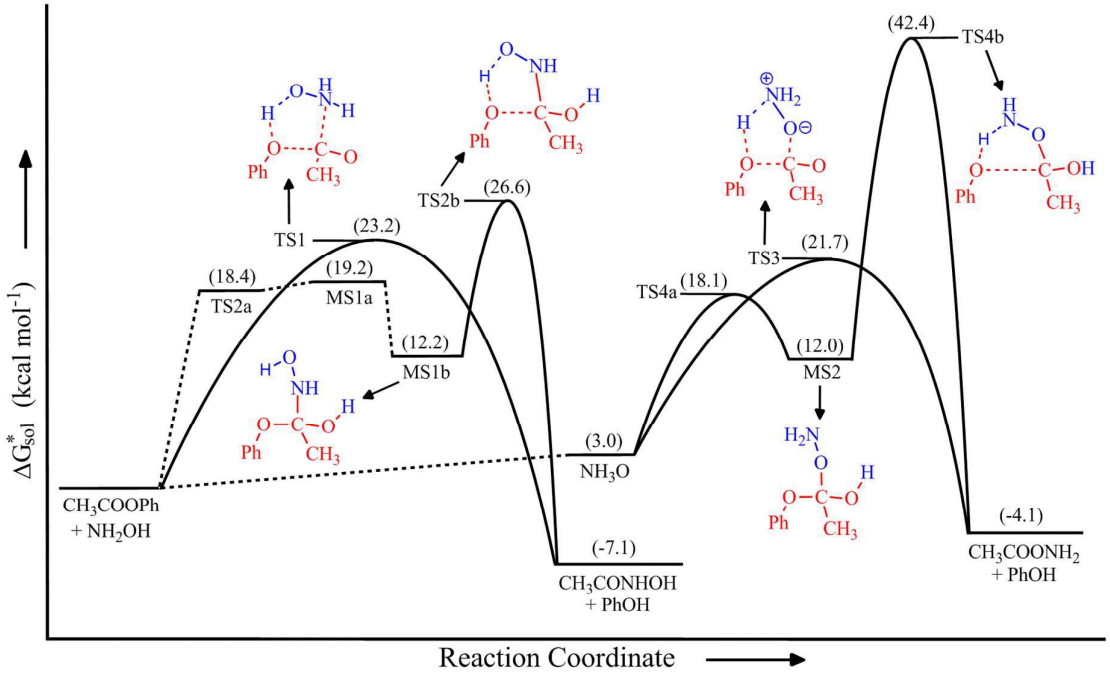

Figure 3: Free energy profile for the reaction of hydroxylamine with phenyl acetate in aqueous solution.

Considering the high solvent effect on the TS1 and mainly on the TS3 structures, we have done a careful analysis of the solvent effect on the geometries and frequencies obtained in the gas phase and in the solution phases with CPCM method using 60, 240 and 960 tesserae. The results are presented in Table 2. The first point to observe is the electronic energy (G_{el}) obtained with the MP4 method calculated on the different geometries. While the values obtained from the gas phase geometries are very different to the solution phase values, the variation of the number of tesserae for obtaining geometries leads to marginal variation of these energies. The most sensible case is TS3, with variation of 0.0006 Hartree. A similar observation can be done for the solvation free energy.

When we observe the G_{VRT} contribution, the values are close for the minimum energy structures. However, for the transition states, they are very sensible to the methodology. Taking the solution phase values with 960 tesserae as the most reliable, we can notice that solution phase calculations with 60 tesserae are the worst values. For example, the error reaches 4 kcal mol^{-1} in the case of TS3. On the other hand, the solution phase values with 240 tesserae are close to solution phase with 960 tesserae for all the structures, but TS1. In this case, the deviation is 0.85 kcal mol^{-1}. Even for gas phase calculations, the G_{VRT} values are close to the reference solution phase with 960 tesserae.

The activation properties for TS1 and TS3 point out the important role of liquid phase optimization and reliable frequency to obtain accurate solution phase activation free energy values. For TS1, underestimation of the gas phase values for $\Delta G^{\ddagger}_{el}$ and $\Delta\Delta G^{\ddagger}_{solv}$ leads to the final $\Delta G^{*\ddagger}_{sol}$ value close to solution phase with 960 tesserae. This cancelation of error does not take place for TS3 and in this case the deviation is as large as 3.30 kcal mol^{-1}. In the case of solution phase with 60 tesserae, the activation barriers are in considerable error. Therefore, this approach should not be used for frequency calculations. In the case of 240 tesserae, the values are much better than 60 tesserae, although the error in $\Delta G^{*\ddagger}_{sol}$ is around 1 kcal mol^{-1} for TS1.

A comparison of the theoretical $\Delta G^{*\ddagger}_{sol}$ with experimental data point out a good performance of the most reliable calculation (solution with 960 tesserae). For TS1, the theoretical value is 23.8 kcal mol^{-1}, just 1.5 kcal mol^{-1} higher than the experimental value. For TS3, the theoretical barrier of 20.8 kcal mol^{-1} is only 0.4 kcal mol^{-1} higher than the experimental value of 20.4 kcal mol^{-1}.

In the global analysis of the free energy profile (Figure 3), we have used solution phase geometry and gas phase frequency. Our study presented in Table 2 suggest this is an reliable and practical approach for predicting free energy barrier in solution, considering the higher computational cost of solution phase frequency with 960 tesserae. In fact, the predicted barriers of 23.2 and 21.7 kcal mol^{-1} for TS1 and TS3, respectively, are in close agreement with the best calculation in this article.

Table 2: Detailed calculations for reaction steps 1 and 3 using different geometries and frequencies in the gas phase and in solution phase.

		NH_2OH	CH_3COOPh	TS1	TS3
Gas	G_{el} [a]	-131.579279	-459.547454	-591.094907	-591.090774
	G_{vrt} [b]	13.20	69.10	93.10	94.49
	ΔG_{solv} [c]	-5.865	-4.720	-17.368	-21.290
Solution Tesserae = 60	G_{el} [a]	-131.541320	-459.359632	-590.867788	-590.860865
	G_{vrt} [b]	12.87	69.38	96.37	98.33
	ΔG_{solv} [c]	-5.930	-5.226	-19.573	-26.767
Solution Tesserae = 240	G_{el} [a]	-131.541328	-459.359581	-590.867600	-590.860445
	G_{vrt} [b]	12.93	69.73	95.12	94.35
	ΔG_{solv} [c]	-5.933	-5.236	-19.779	-27.336
Solution Tesserae = 960	G_{el} [a]	-131.541330	-459.359597	-590.867681	-590.860236
	G_{vrt} [b]	12.99	69.76	94.28	94.39
	ΔG_{solv} [c]	-5.934	-5.238	-19.760	-27.600

Reaction - TS1

	$\Delta G^{\ddagger}_{el}$ [d]	$\Delta G^{*\ddagger}_{g}$ [e]	$\Delta\Delta G^{\ddagger}_{solv}$ [f]	$\Delta G^{*\ddagger}_{sol}$ [g]	EXP. [h]
gas	19.97	30.77	-6.78	23.99	
Tesserae = 60	20.81	34.94	-8.42	26.53	
Tesserae = 240	20.90	33.36	-8.61	24.75	
Tesserae = 960	20.86	32.40	-8.59	23.81	22.3

Reaction - TS3

	$\Delta G^{\ddagger}_{el}$ [d]	$\Delta G^{*\ddagger}_{g}$ [e]	$\Delta\Delta G^{\ddagger}_{solv}$ [f]	$\Delta G^{*\ddagger}_{sol}$ [g]	EXP. [h]
gas	22.56	34.76	-10.71	24.05	
Tesserae = 60	25.16	41.24	-15.61	25.63	
Tesserae = 240	25.39	37.08	-16.17	20.92	
Tesserae = 960	25.53	37.18	-16.43	20.75	20.4

[a] – Electronic contribution to the free energy obtained at single point MP4 method on the optimized geometry (see Computational Methods section). Units in Hartree. All geometries obtained at X3LYP/6-31(+)G(d) or CPCM/X3LYP/6-31(+)G(d) levels. [b] – Vibrational, rotational and translational contribution to the free energy. Units in kcal mol^{-1}. [c] – Single point calculation of the solvation free energy using the SM8 method. [d] Activation electronic energy obtained from single point MP4 calculations. Units in kcal mol^{-1}. [e] – This corresponds to gas phase free energy (electronic, vibrational,

rotational and translational contributions) as defined in the Computational Methods section. Units in kcal mol^{-1}. [f] – Solvation free energy contribution using SM8 method. Units in kcal mol^{-1}. [g] – Solution phase activation free energy. Units in kcal mol^{-1}. [h] – Experimental data from reference 4.

Conclusion

The theoretical calculations reported in this article show that hydroxylamine reacts with phenyl acetate through a single step mechanism, without a tetrahedral intermediate formation, involving both N– and O– attack to the carbonyl center. The O– attack takes place through the zwitterionic form of hydroxylamine and corresponds to the main reaction pathway, with a theoretical free energy barrier of 20.8 kcal mol^{-1}, close to the experimental value of 20.4 kcal mol^{-1}. Both the mechanisms involves transition state stabilization by hydrogen bond involving either the $–NH_3^+$ or –OH group. Other reaction pathways involving tetrahedral intermediates formation are unfavorable. The special feature of hydroxylamine, the high stability of its zwiterionic form, does not occur for hydrogen peroxide neither hydrazine. We believe that this interesting property and reactivity of hydroxylamine functional group should be explored in nucleophilic catalysis. This work complement a previous report, where the catalyzed mechanism was found.[5]

We have also investigated the effect cavity tessellation in CPCM calculations and our results suggest that 60 tesserae is recommended only for geometry optimization, because the respective frequency values may be in considerable error. A cheap and reliable approach is using CPCM for geometries and gas phase frequencies for thermodynamic data estimation.

Acknowledgments

The authors thank the support of the agencies CNPq, FAPEMIG and CAPES.

References

1. W. P. Jencks, *J. Am. Chem. Soc.*, 1958, **80**, 4581-4584.
2. W. P. Jencks, *J. Am. Chem. Soc.*, 1958, **80**, 4585-4588.
3. R. A. Hess, A. C. Hengge and W. W. Cleland, *J. Am. Chem. Soc.*, 1997, **119**, 6980-6983.
4. D. J. Mazera, J. C. Gesser and J. R. Pliego Jr, *Arkivoc*, 2007, 199-214.
5. D. J. Mazera, J. R. Pliego Jr, G. I. Almerindo and J. C. Gesser, *J. Brazil. Chem. Soc.*, 2011, **22**, 2165-2170.
6. A. J. Kirby, J. E. Davies, T. A. S. Brandão, P. F. Silva, W. R. Rocha and F. Nome, *J. Am. Chem. Soc.*, 2006, **128** 12374-12375.
7. A. J. Kirby, J. E. Davies, D. J. Fox, D. R. W. Hodgson, A. E. Goeta, M. F. Lima, J. P. Priebe, J. A. Santaballa and F. Nome, *Chem. Commun.*, 2010, **46**, 1302-1304.
8. M. I. Fernandez, M. Canle, M. V. Garcia and J. A. Santaballa, *Chem. Phys. Lett.*, 2010, **490**, 159-164.
9. G. F. de Lima, J. R. Pliego Jr and H. A. Duarte, *Chem. Phys. Lett.*, 2011, **518**, 61-64.
10. J. R. Pliego Jr, *Theor. Chem. Acc.*, 2011, **128**, 275-283.
11. G. F. de Lima, H. A. Duarte and J. R. Pliego Jr, *J. Phys. Chem. B*, 2010, **114**, 15941-15947.
12. M. Medeiros, E. H. Wanderlind, J. R. Mora, R. Moreira, A. J. Kirby and F. Nome, *Org. Biomol. Chem.*, 2013, **11**, 6272-6284.
13. J. J. A. G. Kamps, R. Belle and J. Mecinovic, *Org. Biomol. Chem.*, 2013, **11**, 1103-1108.
14. X. Xu, Q. Zhang, R. P. Muller and W. A. Goddard III, *The Journal of Chemical Physics*, 2005, **122**, 014105-014114.
15. X. Xu and W. A. Goddard III, *Proccedings of the National Academy of Sciences of the United States of America*, 2004, **101** 2673-2677.
16. V. Barone and M. Cossi, *J. Phys. Chem.*, 1998, **102**, 1195-2001.
17. F. Weigend and R. Ahlrichs, *Phys. Chem. Chem. Phys.*, 2005, **7**, 3297-3305.
18. A. V. Marenich, R. M. Olson, C. P. Kelly, C. J. Cramer and D. G. Truhlar, *J. Chem.Theory Comput.*, 2007, **3**, 2011-2033.
19. J. R. Pliego Jr and W. B. de Almeida, *J. Phys. Chem. A*, 1999, **103**, 3904-3909.
20. D. G. Truhlar and J. R. Pliego Jr, in *Continuum Solvation Models in Chemical Physics: From Theory to Applications* eds. B. Mennucci and R. Cammi, Wiley-VCH, 2007, pp. 338-365.
21. Y. Y. Chuang, C. J. Cramer and D. G. Truhlar, *Int. J. Quant. Chem.*, 1998, **70**, 887-896.
22. A. A. Granovsky, Firefly version 7.1.F, http://classic.chem.msu.su/gran/gamess/index.html.
23. M. W. Schmidt, K. K. Baldridge, J. A. Boatz, S. T. Elbert, M. S. Gordon, J. H. Jensen, S. Koseki, N. Matsunaga, K. A. Nguyen, S. Su, T. L. Windus, M. Dupuis and J. A. Montgomery Jr, *J. Comp. Chem.*, 1993, **14**, 1347-1363.
24. M. Higashi, A. V. Marenich, R. M. Olson, A. C. Chamberlin, J. Pu, C. P. Kelly, J. D. Thompson, J. D. Xidos, J. Li, T. Zhu, G. D. Hawkins, Y.-Y. Chuang, P. L. Fast, B. J. Lynch, D. A. Liotard, D. Rinaldi, J. Gao, C. J. Cramer and D. G. Truhlar, *GAMESSPLUS - version 2010-2*, (2010) University of Minnesota, Minneapolis.

25. Y. S. Simanenko, A. F. Popov, T. M. Prokopeva, E. A. Karpichev, V. A. Savelova, I. P. Suprun and C. A. Bunton, *Russ. J. Org. Chem.*, 2002, **38**, 1341-1353.
26. Y. S. Simanenko, A. F. Popov, T. M. Prokop'eva, V. A. Savelova and I. A. Belousova, *Theor. Exp. Chem.*, 1994, **30**, 61-64.
27. T. A. Nigst, A. Antipova and H. Mayr, *J. Org. Chem.*, 2012, **77**, 8142-8155.
28. P. L. da Silva, L. Guimaraes and J. R. Pliego, *J. Phys. Chem. B*, 2013, **117**, 6487-6497.